Building the central Andes through axial lower crustal flow

William B. Ouimet[1] and Kristen L. Cook[2]

Received 9 February 2009; revised 14 August 2009; accepted 4 January 2010; published 11 June 2010.

[1] The orogen-scale morphology of the central Andes, which are longitudinally symmetric at ~19°S, correlates with the modern geometry of the subducting Nazca slab but is largely independent of local bedrock geology or precipitation. Crustal thickness, as measured by the cross-strike width of the orogen above 3000 m and the cross-sectional area of the crust, is not well correlated with observed magnitudes of upper crustal shortening. In our interpretation, the large-scale morphology is instead correlated with and controlled by lithospheric-scale processes and subduction dynamics. Using a semi-analytic, three-dimensional Newtonian viscous flow model, we produce Andean-like topography and distribution of upper crustal shortening during subduction of an oceanic lithosphere eastward beneath the Andes provided that (1) the more steeply dipping slab segment beneath the central Andes is overlain by the weak lower or middle crust, (2) the flat slab subduction segments to the north and south of this zone are overlain by the strong middle and lower crust, and (3) the steeply dipping central slab segment is overlain by a narrow, centrally localized zone of increased crustal shortening. The resulting model orogen displays substantial orogen-parallel flow in the weak lower crust above the steep slab zone. Orogen-parallel flow does not penetrate into the regions of stronger lower crust above the flat slab segments, resulting in a broad, plateau-topped orogen above the central slab segment and narrow but high orogenic segments above the flat slab region. Redistribution of material through lower crust flow can account for the observed mismatch between crustal volume and upper crustal shortening in the central Andes and may explain young (<10 Ma) crustal thickening and surface uplift that has been argued for in some regions. **Citation:** Ouimet, W. B., and K. L. Cook (2010), Building the central Andes through axial lower crustal flow, *Tectonics*, *29*, TC3010, doi:10.1029/2009TC002460.

1. Introduction

[2] The development of high topography in the central Andes, including development of the Altiplano and Puna plateaus, has resulted from Tertiary shortening of the South American plate during eastward subduction of the Nazca plate beneath South America [*Isacks*, 1988]. The mechanisms that contribute to crustal thickening and surface uplift remain enigmatic, and much of the plateau exhibits a mismatch between crustal volume and estimates of upper crustal shortening. The thick crust and high topography in the northern Altiplano and the Puna coincide with significant deficits in measured upper crustal shortening [*Kley and Monaldi*, 1998], while the central Altiplano coincides with substantially more upper crustal shortening, perhaps even an excess [*McQuarrie*, 2002]. The central Andes also display a remarkable symmetry in orogen width and cross-sectional area, despite a pronounced asymmetry in precipitation and upper crustal lithology. The transition from a wide plateau to a narrower mountain range to both the north and south of the Altiplano coincides with changes in the modern dip of the subducting Nazca slab, from a steeply dipping slab underneath the Altiplano to a flat slab underneath the regions to the north and south. Such observations suggest that the overall morphology of the central Andes is largely independent of local geology, upper crustal shortening, and precipitation and may be largely controlled by orogen-scale dynamics of the lithosphere and underlying subduction systems.

[3] Lower crustal flow has been proposed to explain crustal thickening and surface uplift in the absence of upper crustal shortening in a number of orogens, most notably beneath the eastern Tibetan Plateau and its margins [*Clark and Royden*, 2000]. Some authors have proposed that in the central Andes, ductile flow within the lower crust redistributes crustal material along strike, translating material away from areas with greater magnitudes of upper crustal shortening and toward areas with lesser magnitudes of upper crustal shortening [*Kley and Monaldi*, 1998; *Hindle et al.*, 2005]. Mass transfer in the lower crust has also been cited as a potential explanation for crustal thickening and surface uplift in the eastern Cordillera of the Bolivian Andes and in the western Altiplano of southwest Peru starting at ~10 Ma [*Barke and Lamb*, 2006; *Schildgen et al.*, 2007]. In this paper, we explore the potential role of lower crustal flow in controlling the morphology and development of high topography in the central Andes.

2. Central Andes (12°S–30°S)

[4] The Andes mountains define the western edge of South America. The orogen is more than 8000 km long and displays large along-strike variations in width, mean elevation, geomorphic character, and style of upper crustal deformation. The highest and widest parts of the orogen are in the central Andes between 12°S and 30°S, culminating in the Altiplano-Puna plateau of southern Peru, Bolivia, and northern Chile (Figure 1). In this region, average elevations

[1]Department of Geology, Amherst College, Amherst, Massachusetts, USA.
[2]Department of Geosciences, National Taiwan University, Taiwan.

0278-7407/10/2009TC002460

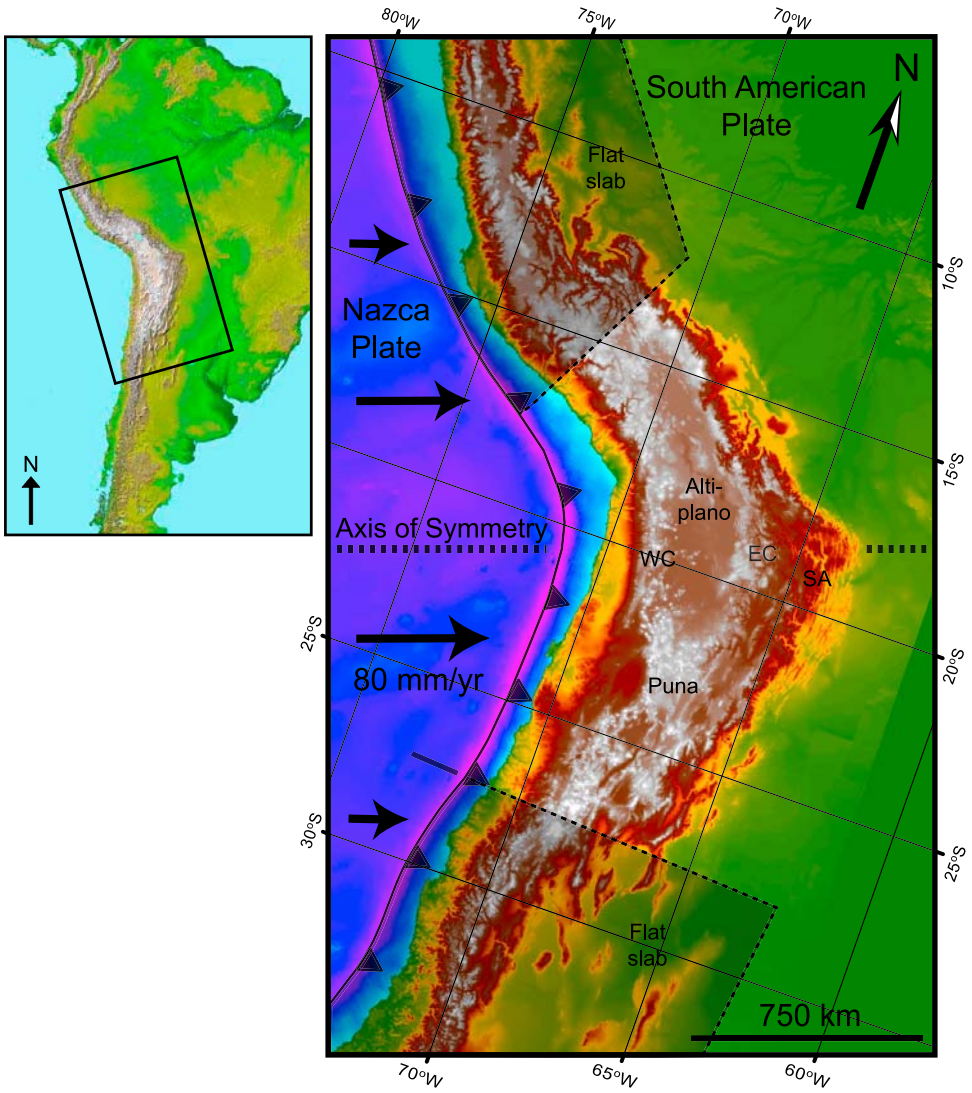

Figure 1a. Topography of the central Andes (GTOPO30) and Pacific Ocean bathymetry (ETOPO5) rotated, such that the dominant plate convergence direction for the past 25 Myr is oriented left/right to illustrate the large-scale symmetry in the topography. Note the shaded regions of flat slab subduction bounding the northern and southern margins of the central Andes, accentuating the symmetry. The axis of symmetry is at ~19°S. WC, Western Cordillera; EC, Eastern Cordillera; SA, sub-Andean Ranges.

of 3.5–4 km persist over an area of ~600,000 km^2 (300 km × 2000 km) [*Isacks*, 1988]; maximum orogen widths are on the order of 600–700 km, and crustal thicknesses are as large as 60–70 km [*Beck et al.*, 1996]. The highest elevations throughout this region are typically mountain peaks associated with Cretaceous-Tertiary volcanic rocks, which rise above the plateau to elevations greater than 6000 m.

[5] The Altiplano-Puna plateau, together with the Western Cordillera, an active volcanic arc, and the Eastern Cordillera, a Tertiary thrust belt, defines a broad zone with average elevation greater than 3000 m (Figure 1). Near ~19°S, the central Andes reach maximum width. Here the eastern margin of the Andes includes the sub-Andean zone, an active, thin-skinned fold-thrust belt, and is bordered by an active foreland basin in the Chaco plain. In the northern Altiplano (~14°S) and in the southern Puna (~28°S), the plateau and cordillera are less well defined. This coincides with a transition to different styles of deformation postulated to result from the presence of flat slab subduction beneath the northern and southern parts of the orogen [*Isacks*, 1988]. From 2°S to ~14°S and 28°S to 34°S, the Nazca plate subducts shallowly beneath the Andes (at <10°). This contrasts with subduction beneath the central Andes, where the Nazca plate subducts at a steeper angle (~30°) [*Jordan et al.* 1983; *Isacks*, 1988; *Cahill and Isacks*, 1992]. These dips reflect the modern subduction geometry of Nazca slab; throughout the Cenozoic this geometry has undergone changes. It has been suggested that the central Andes were underlain by shallow-angle

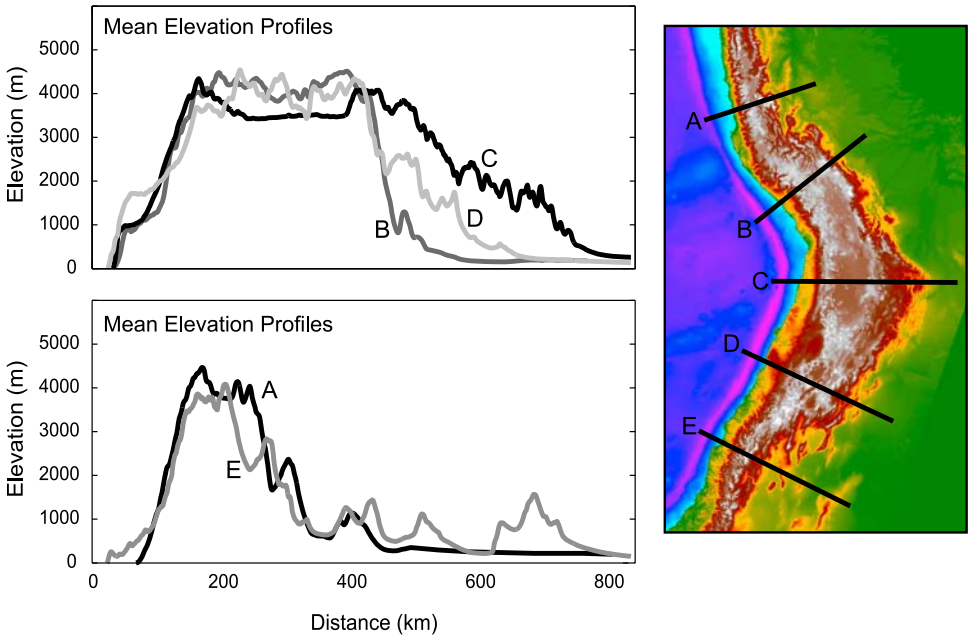

Figure 1b. Comparison of cross sections at analogous locations north and south of the axis of symmetry. Note the similarities in width and elevation.

subduction prior to steepening in the last 25 Myr [*Isacks*, 1988], and the present-day shallow-angle subduction south of the Altiplano is argued to have developed only in the last 5–10 Myr, in associated with an oceanic ridge on the Nazca plate being subducted beneath South America [*Ramos et al.*, 2002].

[6] The timing of shortening, crustal thickening, and surface uplift in the central Andes remains enigmatic. Early studies suggested that the deformation and crustal thickening responsible for building the central Andes occurred largely during the past 25 Myr [*Isacks*, 1988; *Allmendinger et al.*, 1997], but more recent studies have documented that a significant amount of the shortening, particularly in the eastern Cordillera, occurred between 40 and 20 Ma [*Gillis et al.*, 2006; *Ege et al.*, 2007; *McQuarrie et al.*, 2008; *Barnes et al.*, 2006]. Exactly when the uplift responsible for the high topography of the Andes observed today occurred, however, continues to be debated. A growing number of studies indicate that a significant part of the Andes began to be uplifted at ~10 Ma [*Lamb and Hoke*, 1997; *Gregory-Wodzicki*, 2000; *Barke and Lamb*, 2006; *Garzione et al.*, 2006; *Ghosh et al.*, 2006; *Schildgen et al.*, 2007], but there are also many studies that suggest uplift occurred prior to 10 Ma [*Gubbels et al.*, 1993; *McQuarrie*, 2002; *Victor et al.*, 2004; *Elger et al.*, 2005; *Ehlers and Poulsen*, 2009].

[7] In the vicinity of the central Andes, the present rate of convergence between the Nazca and South American plates is ~8 cm/yr (NUVEL-1A [*DeMets et al.*, 1994]). Shortening estimates from GPS data in the sub-Andean zones are ~1.5–2 cm/yr [*Norabuena et al.*, 1998]. The pre-Tertiary crustal thickness is believed to have been ~30–35 km, requiring an approximate doubling of the crust to reach the current crustal thickness of the central Andes [*Sempere et al.*, 2002].

2.1. Estimates of Upper Crustal Shortening

[8] The cross-sectional area and orogen widths observed in the central Andes are inconsistent with current estimates of upper crustal shortening. Structures that accommodate shortening vary along strike (Figure 2). The sub-Andean thrust belt, which accommodates much of the shortening in the central part of the Bolivian orocline, disappears to the south, where it is replaced by a series of uplifted basement blocks. To the north, the sub-Andean thrust belt narrows and disappears into an undifferentiated package of sedimentary rocks metamorphosed to low grade. This makes it difficult to measure accurately the total magnitude of upper crustal shortening. Near the axis of symmetry in the central Altiplano between 17°S and 22°S, many researchers have documented large magnitudes of upper crustal shortening (200–300 km), with some estimates reaching as high as ~530 km [*Kley and Monaldi*, 1998; *McQuarrie*, 2002]. The higher estimates suggest that there may be an excess of upper crustal shortening in the central Altiplano (see Figure 3g), but because of the wide range of shortening estimates for this region, the degree to which there is an excess amount is debated. In contrast, measured shortening estimates in the Puna, between 22°S and 28°S, range from 70 to 120 km. In the northern Altiplano, between 17°S and 14°S, the few existing estimates are even lower, suggesting only ~50 km of shortening [*Kley and Monaldi*, 1998].

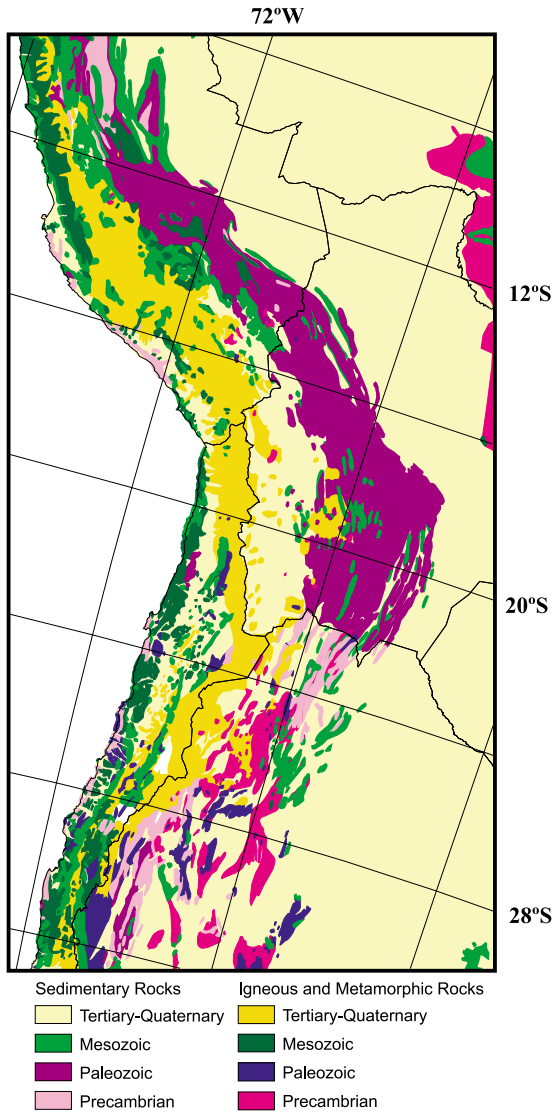

Figure 2. Simplified geologic map of the central Andes. Geology generalized from *Schenk et al.* [1998].

[9] The small magnitude of apparent upper crustal shortening in the northern and southern sections of the central Andes is not sufficient to explain current crustal thicknesses (>50 km) and orogen widths (>300 km) observed here (Figure 3), which correspond to more than ~200 km of upper crustal shortening. We therefore see a mismatch between crustal volume and upper crustal shortening throughout the plateau, with a substantial amount of shortening in the center of the Altiplano (possibly an excess), and a deficit in the northern Altiplano and Puna (Figure 3g). We use the pattern of measured shortening to support a model setup that includes a narrow, localized zone of increased crustal shortening in the middle part of the central Andes near the axis of symmetry. We also consider that there could indeed be an "excess" amount of shortening in the central Andes, even though this is not agreed upon in the literature. One alternative explanation for this apparent excess is that the felsic composition of the crust underlying the central Altiplano could have resulted from mafic lower crust turning to eclogite and foundering, thus accounting for some of the excess thickened crust [*Babeyko et al.*, 2002].

2.2. Orogen Morphology

[10] The longitudinal symmetry of the Andes can be observed visually (Figure 1) but is highlighted by quantitative analysis of topographic swath profiles constructed perpendicular to the trench (Figures 1b and 2) [also see *Isacks*, 1988]. The profiles show maximum, minimum, and mean elevations averaged across 80 km wide swaths. Using the mean topography from each swath profile, we compiled the cross-sectional area (area under the mean topography profile and above sea level), the orogen width at 3000 m elevation, and the highest mean elevation (Figure 3). The along-strike symmetry in cross-sectional area and orogen width is clear when compared to the same data inverted about the axis of symmetry (at ~19°S, where cross-sectional area and orogen width are a maximum). North and south of 19°S, cross-sectional area and orogen width are relatively uniform above the region of steeper slab subduction (from ~14°S to 28°S). At the transition to flat slab subduction to the north and south, there is a pronounced decrease in these values. The maximum peak elevations are largely invariant along the length of the orogen and appear unrelated to underlying slab geometry. Relatively small, local variations in width and cross-sectional area, such as occur around 16°S, are probably related to local processes but do not significantly affect the large-scale symmetry of the orogen or the clear changes in width and cross-sectional area that occur near 14°S and 28°S. It is likely that the local variations in orogen morphology are related to variable precipitation and drainage patterns along strike.

2.3. Regional Bedrock Geology and Structure Style

[11] The bedrock geology and style of structural deformation on the eastern flanks of the Andes vary significantly along-strike and are highly asymmetric (Figure 2) [*Allmendinger et al.*, 1997; *Schenk et al.*, 1998]. The northern region is composed mostly of low-grade Paleozoic metasediments, with a small amount of Precambrian and Mesozoic metasediments in a few locations. The central region is dominated by a thick sequence of Paleozoic sedimentary rocks that make up the thin-skinned sub-Andean fold-thrust belt. The southern region is distinguished by Precambrian basement rocks and Paleozoic intrusives deformed in a thick-skinned thrust belt [*Schenk et al.*, 1998]. The geology west of the Eastern Cordillera is more consistent along strike. Most of the plateau region is covered by Quaternary sediments and Cretaceous to Tertiary volcanic rocks. Mesozoic to Cenozoic intrusive rocks are found mainly in the coastal cordillera to the west of the Western Cordillera and in the northern peaks of the central Andes.

2.4. Annual Precipitation

[12] Annual precipitation in the central Andes is also highly asymmetric (Figure 3f) and varies along strike by an order of magnitude. The highest values occur on the steep topographic escarpment abutting the northeastern edge of

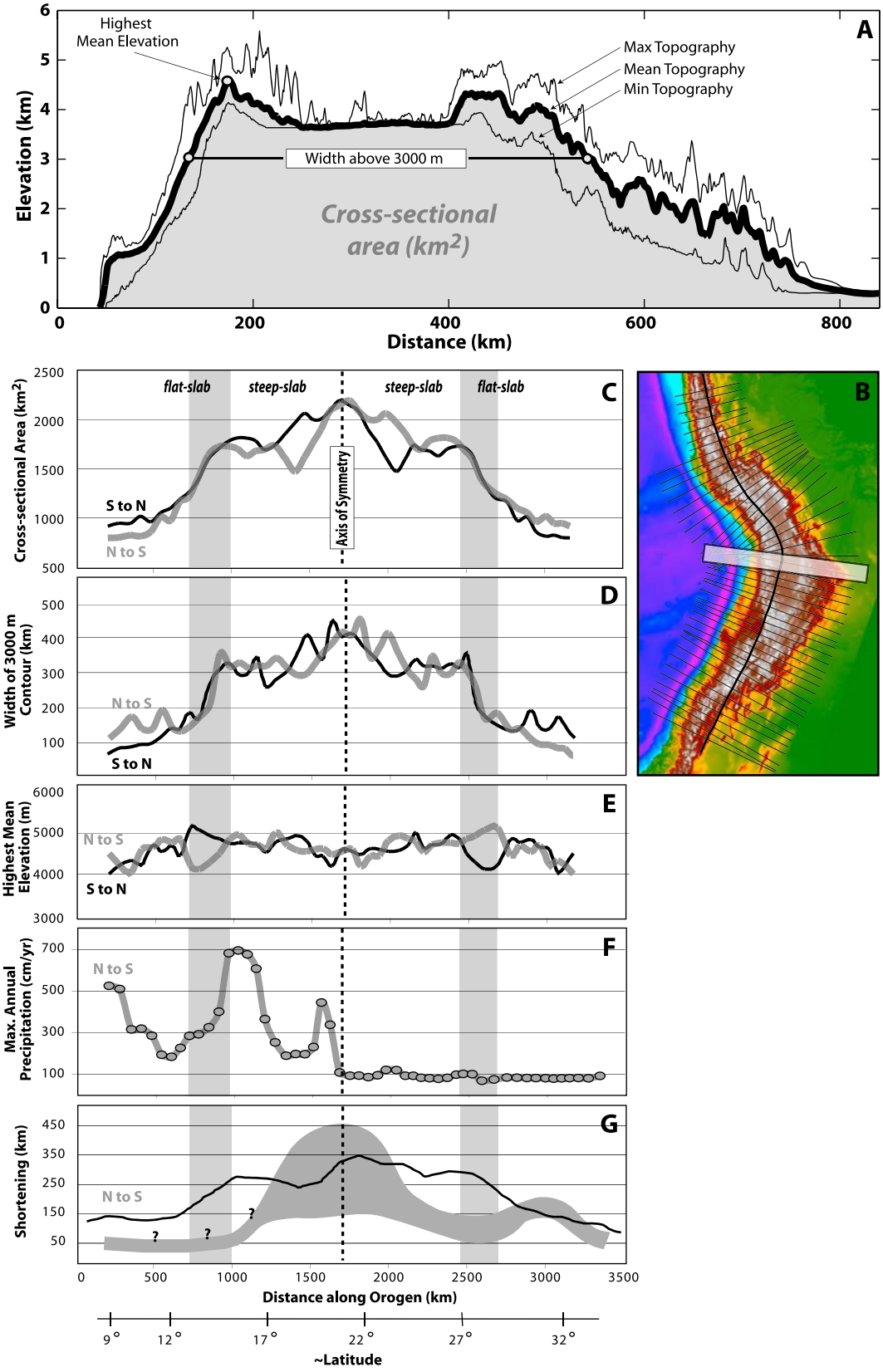
A
Highest
Mean Elevation
Max Topography
Mean Topography
Min Topography
Width above 3000 m
Cross-sectional
area (km2)
Elevation (km)
Distance (km)
B
C
flat-slab
steep-slab
steep-slab
flat-slab
Axis of Symmetry
S to N
N to S
Cross-sectional Area (km2)
D
Width of 3000 m
Contour (km)
E
Highest Mean
Elevation (m)
F
Max. Annual
Precipitation (cm/yr)
G
Shortening (km)
Distance along Orogen (km)
~Latitude
9°
12°
17°
22°
27°
32°

Figure 3

the plateau in Peru and Bolivia (centered on 15°S–17°S), and low values occur in all other areas of the plateau and associated high topography [*Peterson and Vose*, 1997] (Figure 3f). Some studies have suggested that increased erosion in areas of high precipitation in the Andes has affected the geomorphic, metamorphic, and structural characteristics of the orogen [*Masek et al.*, 1994; *Horton*, 1999; *Montgomery et al.*, 2001], but variations in precipitation do not appear to significantly affect the large-scale morphology of the central Andes, particularly at elevations above 3000 m.

3. Crustal Flow Modeling

[13] The data summarized above suggest that the topography of the central Andes is tied primarily to the dynamics and modern geometry of the Nazca/South America subduction boundary rather than to variations in properties such as surface geology or climate. This conclusion, originally discussed and argued by *Gephart* [1994], motivates us to consider processes that may relate slab geometry and crustal strength variations to morphology via crustal deformation and whether these processes could explain the shortening deficit, described above, of the Puna and northern Altiplano.

[14] The role of the lower crust in the development of orogenic plateaus has been discussed in the context of the Altiplano [*Kley and Monaldi*, 1998; *Hindle et al.*, 2005; *Husson and Sempere*, 2003; *Yang et al.*, 2003] and the Tibetan Plateau [*Bird*, 1991; *Royden*, 1996; *Beaumont et al.*, 2006], as well as in theoretical models of plateau development [*Vanderhaeghe et al.*, 2003]. Central to this discussion is the assumption that the crust may, under appropriate conditions, become weak enough to enable ductile channel flow in response to lateral pressure gradients resulting from variations in crustal thickness. This enables a lateral flux of deep crustal material beneath the plateau with minimal deformation of the upper crustal layer and may effectively decouple the motion of the upper crust from that of the mantle. Experimental, observational, and theoretical studies suggest that the strength of continental crust can decrease significantly at high temperatures and/or in the presence of fluids or partial melt [*Kohlstedt et al.*, 1995; *Rosenberg and Handy*, 2005].

[15] Previous modeling studies of lower crustal flow in the Andes have focused on east-west lower crustal flow from Eastern and Western cordilleras into the Altiplano [*Husson and Sempere*, 2003] or have examined only north to south lower crustal flow with a prescribed geometry for the Andes topography and an imposed distribution of deformation [*Yang et al.*, 2003]. Our approach employs a three-dimensional viscous flow model to explore the relationships between slab dip, crustal strength, lower crustal flow, and the topography, uplift, and orogen-scale symmetry of the central Andes.

3.1. Model Framework

[16] The modeling approach adopted in this paper is identical to that of *Cook and Royden* [2008] [see also *Royden*, 1996; *Shen et al.*, 2001]. The crust is treated as an idealized incompressible Newtonian viscous fluid with two layers representing the upper and lower crust. Viscosity is allowed to vary laterally in both layers but is depth invariant within each layer. Deformation is fully described by the Stokes and continuity equations. With appropriate boundary conditions, we obtain analytical expressions for velocity at the surface of the crust and the change in crustal thickness over time at length scales that are similar to and longer than the thickness of the crust. A detailed discussion of the methods, parameters, and assumptions is given by *Cook and Royden* [2008].

[17] In this study, we do not model the thermal state of the crust explicitly. The relationship between temperature and the bulk strength of the crust is neither straightforward nor well constrained, requiring assumptions about composition, hydration, and temperature at depth. Instead, the model specifies the viscosity in the lower crust directly as a response to the evolving crustal thickness. Initially, the crust has a uniform viscosity throughout; when it thickens beyond a specified value, the viscosity of the lower crust is reduced as the lower crustal layer thickens and is a function of crustal thickness. Once the total crustal thickness reaches a critical value, the viscosity stabilizes at a prescribed minimum value. If the crust subsequently thins to be less than this critical value, the viscosity of the lower crust is again allowed to depend on crustal thickness, increasing as the crust thins. Alternatively, viscosity of the lower crust can be keep constant during thickening and never lower. The implication being that some crustal columns are relatively weak, susceptible to a lowering of viscosity during crustal thickening, while others are strong, able to keep a high viscosity despite increasing temperature during crustal thickening.

Figure 3. Topographic analysis of the central Andes. (a) Example of one of the topographic swath profiles used in our analysis (cross section 27, at ~19°S), showing how cross-sectional area, width, and peak elevations were calculated. The topographic data used for all swaths are GTOPO30 data, 888 m grid spacing. The profiles for maximum, minimum, and mean elevations are based on a 80 km wide window. (b) Location and key for 59 topographic swath profiles, showing the axis (parallel to the trench) from which profiles were extracted perpendicularly. Profiles were analyzed to investigate specific trends along the orogen length, such as (c) cross-sectional area above sea level, (d) width of the 3000 m contour, and (e) highest mean elevation. Shaded regions on each plot are the respective beginnings of the flat slab regions. Each trend is plotted N-S and flipped S-N at the axis symmetry. (f) Plot showing maximum annual precipitation variation along strike, N-S. Maximum annual precipitation values were calculated from swaths of precipitation data equal in extent to the topographic swaths. The interpolated DEM of peak annual precipitation (not shown) was derived from GHCN Version 2 Global Precipitation data set [*Peterson and Vose*, 1997]. (g) Shortening estimates along strike, N-S. Gray shading indicates the range of shortening estimates based on geologic data; black line indicates the amount of shortening expected based on cross-sectional area [after *Kley and Monaldi*, 1998, Figure 2].

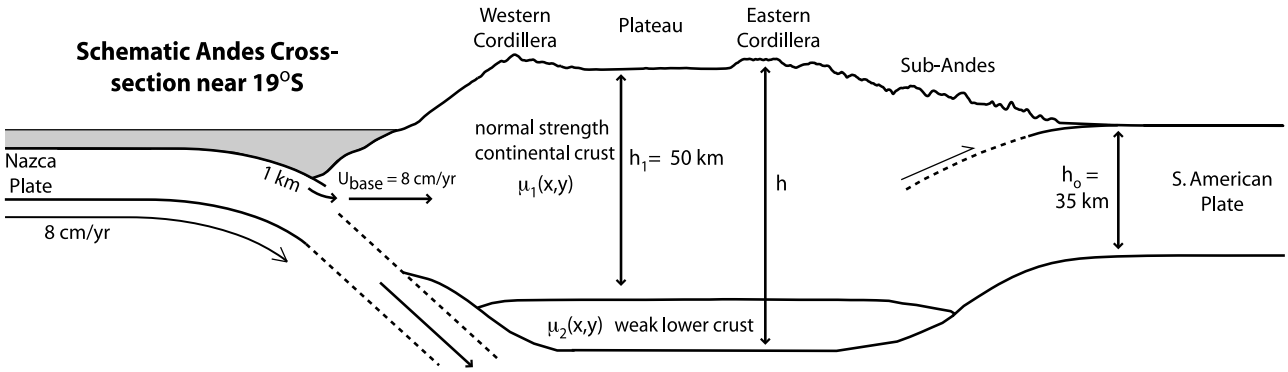

Figure 4. Schematic cross section of the Andes at ~19°S showing basic parameters used in the model (crustal thicknesses, viscosities, convergence velocities, etc.).

3.2. Model Setup

[18] A schematic cross section (Figure 4) illustrates the setup and parameters used in this study. Crustal deformation is driven by "plate-like" mantle velocities imposed at the base of the crust. Topography evolves in response to the interaction between this forcing and the pressure gradients created by the evolving topography itself. Isostatic equilibrium is assumed everywhere. We present topography in our model results instead of crustal thickness simply because the topography of the Andes is better constrained and easier to visualize. We assume a uniform initial continental crustal thickness of 35 km and an initial oceanic crustal thickness of 1 km. The 1 km of oceanic crust represents an estimate of material incorporated into the Andean orogen from the subducted slab while the rest of the oceanic crust is subducted. The incorporation of oceanic crust into the modeled South American plate is required for model stability, and the converging oceanic crust must have a nonzero thickness. The crust is assigned an initial viscosity of 10^{21} Pa s. We explore crustal strength variations along the modeled Andean margin by specifying which regions of the South American plate are allowed to weaken and achieve lower viscosity values (as low as 10^{17} Pa s) during crustal thickening.

[19] Crustal thickening within the South American plate is imposed on the model by assigning westward motion (underthrusting) to the South American plate and by advancing the subduction zone eastward through time. The resulting convergence of continental crust represents deformation (i.e., shortening) within the South American plate above the subduction zone. In the model, the subduction zone advances eastward through time by assigning a positive (eastward) velocity to the base of the continental crust at the subduction boundary, and underthrusting of the South American plate is accomplished by assigning a negative (westward) velocity to the base of the entire South American plate. In most regions, the velocity of the advancing subduction zone is 0.75 cm/yr, while the South American plate velocity is −1.5 cm/yr. More rapid eastward motion of the advancing subduction zone (up to 3.75 cm/yr) and slightly more rapid westward underthrusting of the South American plate (up to −3 cm/yr) are applied to the region that will develop into the center of the Bolivian orocline, enhancing the shortening of the South American plate in this region (e.g., Figure 5b). We refer to this zone as the orocline zone. The subduction boundary is not straight, and convergence is specified to be parallel to the axis of symmetry, which is similar to the observed direction of convergence between the Nazca and South American plates (Figure 1). The total far-field convergence between the Nazca plate and South American plate in the model is specified at 8 cm/yr. This 8 cm/yr of total convergence gets balanced along the modeled Andean margin by the velocities imposed at the base of the crust, such that velocities underlying the Nazca plate range from 5 to 6.5 cm/yr and velocities underlying the South American plate range from −1.5 to −3 cm/yr.

3.3. Model Results

[20] We evaluated many different subduction zone geometries, basal velocities, shortening patterns, and viscosity structures before arriving at the model results illustrated in Figures 5–9. The most Andean-like results occur with a subduction boundary that is divided into several regions related to the modern slab geometry (Figure 5b). In the orogenic segment underlain by a more steeply subducting slab (between 14°S and 28°S), the viscosity of the lower crust begins to drop when the crust reaches a thickness of 50 km and arrives at its minimum value of 10^{17} Pa s when the crust reaches a thickness of 65 km. In the orogenic segments underlain by flat slab subduction (north of 14°S and south of 28°S) the lower crust is not allowed to weaken, and the viscosity remains uniform throughout the crust. Embedded in the center of the steep slab zone is a narrower oroclinal zone where there is more shortening within the South American plate than to the north and south (while total convergence remains uniform). This corresponds to the area where the eastward advance of the Nazca subduction boundary is more rapid than in the areas to the north and south and where the magnitude of westward underthrusting of the South American plate is also greater. The more rapid underthrusting of the South American plate in the center of the orogen results in greater crustal thickening in this region, as more continental lithosphere is incorporated into the orogen from the east. This

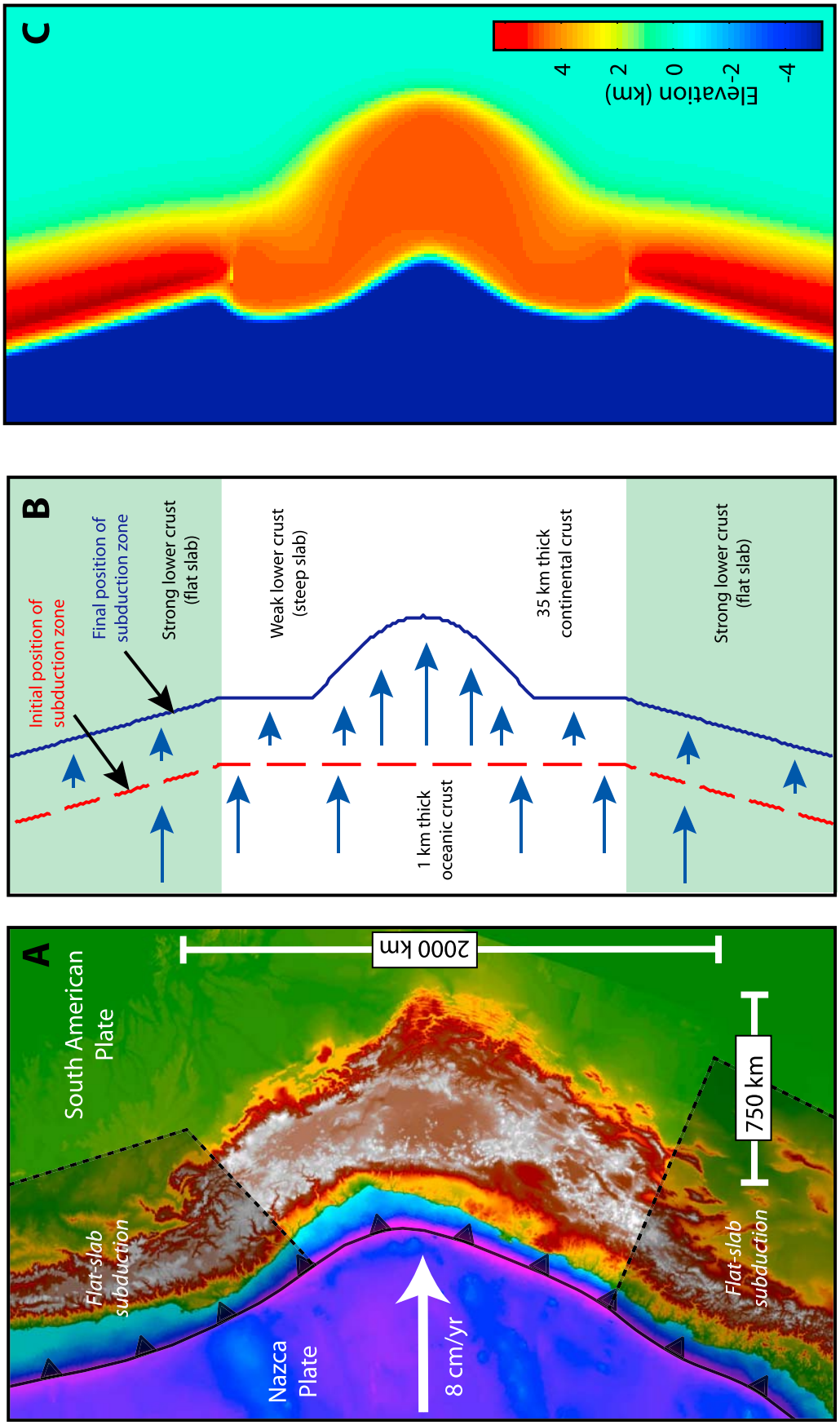

Figure 5. Boundary conditions and model setup motivated by topography symmetry and geometry of the Nazca/South America subduction zone boundary. (a) Topographic symmetry. (b) Plan view model setup. (c) Model topography after 30 Myr. Flat slab zones are modeled as strong crust where no lower crustal flow occurs. Shortening is focused at the center of the Bolivian orocline. Deformation is driven by moving the subduction zone to the east and by underthrusting the South American plate to the west; note the initial and final positions of the subduction zone boundary.

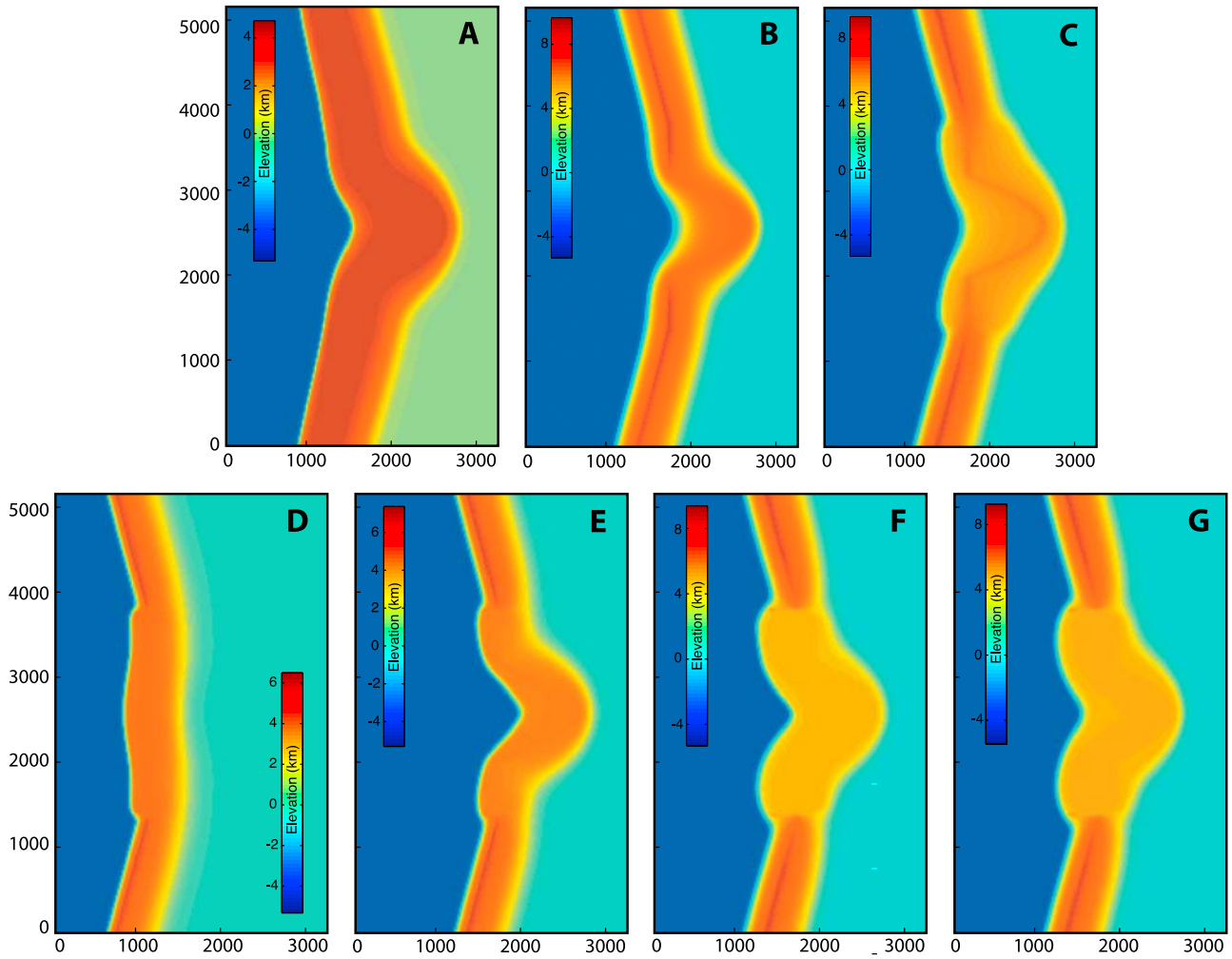

Figure 6. Examples of model setup yielding non-Andean-like results. Note the different scale bars. All runs use the same model parameters as indicated in Table 1, except for the following differences. (a) The lower crust is allowed to weaken everywhere (i.e., there are no flat slab zones with uniform viscosity); a plateau forms everywhere. (b) The lower crust everywhere remains strong (and viscosity never lowers); a plateau does not develop in the central Andes. (c) The lower crust in the center is allowed to weaken slightly, to 10^{20} Pa s; a wider orogen forms, but a plateau does not develop. (d) The subduction zone boundary does not advance. (e) No westward motion is assigned to the South American plate; this results in too little shortening in the center of the orogen. (f) A uniform westward motion is applied to the South American plate; again there is too little shortening in the center of the orogen. (g) The oceanic crust has a thickness of only 100 m; there is little effect on the resulting orogen (compared to Figure 5c).

model setup effectively generates topography with morphology generally similar to that of the central Andes (Figure 5c). For a full list of the model parameters related to this preferred model setup, see Table 1.

[21] The seven addition model runs presented in Figure 6 highlight the sensitivity of our most Andean-like results to changing key model parameters. These additional runs include model setups that have different subduction zone geometries and associated viscosity structures (Figures 6a, 6b, and 6c), a nonadvancing subduction zone (Figure 6d), no underthrusting of the South American plate (Figure 6e), uniform underthrusting of the South American plate (i.e., no zone of increased underthrusting in the center) (Figure 6f), and a much thinner oceanic crust (Figure 6g). Each model result, in its own way, produces topography that is not as Andean as that generated from the preferred model setup discussed above (see Figure 6 caption for more details). These additional runs emphasize that our model produces Andean-like topography provided that (1) the more steeply dipping slab segment beneath the central Andes is overlain by weak lower or middle crust, (2) the flat slab subduction segments to the north and south of this zone are overlain by strong middle and lower crust, and (3) the steeply dipping central slab segment is overlain by a narrow, centrally localized zone of increased crustal shortening.

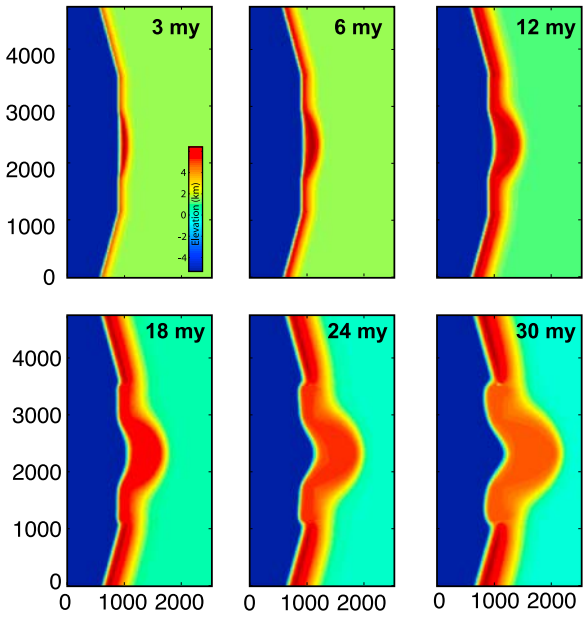

Figure 7. Time series depicting the evolution of topography during one model run for 30 Myr. Model time 3 Myr refers to 27 Ma before present, 18 Myr refers to 12 Ma before present, and so on. Each image represents a DEM of elevations. Scale bars evolve to the final scale bar shown in model time 30 Myr (present-day).

[22] The increased magnitude of crustal shortening along the eastern side of the central orocline region in our most Andean-like results is accommodated by orogen-parallel flow of deep crust to the north and south. Orogen-parallel flow is restricted to the area of weak lower crust, and hence to the hotter crust above the zone of steeper subduction. Because the lower crust does not weaken until the crust reaches a prescribed critical thickness, there is little axial flow of crust during the initial stages of orogen growth. As the crust in the steep slab region reaches the prescribed critical crustal thickness, the lower crustal viscosity decreases, and deep crustal material flows away from the central region of highest shortening toward the north and south. This results in a redistribution of crust as illustrated by cross sections extracted from model topography (Figures 8 and 9).

[23] Flow within the low-viscosity crustal layer occurs under low-pressure gradients, so that flow within the weak crust region continues until the elevation above the weak crust region is the nearly the same along and across strike (Figure 9). As the lower crust flows northward and southward from the center of the orogen, the cross-sectional width and integrated topography across the model orogen also become similar throughout the weak crust region. Thus, the amount of crust added to the orogen, as estimated from the cross-sectional area of the orogen, is similar along the entire weak crust region of the orogen despite the fact that central part of the weak crust region experiences ~3 times as much upper crustal orogen-perpendicular shortening as the weak crust regions to the north and south (Figure 10). This is consistent with observations from the Andes, where crustal shortening estimates above the steep slab region are much higher between 17°S and 22°S (>300 km) and much lower to the north (<50 km) and south (70–120 km) [e.g., *Kley and Monaldi*, 1998].

4. Discussion

[24] Our results suggest that the large-scale morphology of the central Andes can be mostly explained by the interaction between subduction geometry and large-scale variations in upper crustal shortening along the length of the Andean belt. Figure 3 shows that this large-scale morphology reflects the modern dip of the subducting slab but is largely insensitive to variations in local shortening, lithology, and precipitation. Within the orogen, a plateau with little along-strike variation in width and cross-sectional area develops as the lower crust weakens above the steeply dipping segment of the Nazca slab, while flow into the region above the flat slab segments is blocked by the presence of a strong lower crust. The redistribution of crust into areas north and south of central orocline zone leads to crustal thickening and surface uplift in the absence of significant shortening that occurs later in the orogen's evolution, consistent with young (<10 Ma) crustal thickening and surface uplift that has been argued for part of the Andes [e.g., *Barke and Lamb*, 2006; *Schildgen et al.*, 2007].

[25] In this paper, our goal is not to produce a replica of the central Andes, in geometry nor in temporal evolution, but rather to gain insight into the role of the deep crustal in the development of large-scale morphology and its relationship to subduction dynamics and lithospheric rheology. The model presented here is simplified as compared to the Andean orogen and ignores much of the complexity of crustal processes and regional geology. It represents a possible end-member model meant to highlight the importance of a single process in orogen development. For example, we have not fine-tuned the model topography above the flat slab zones, where the orogen is narrow and steep; the high model elevations in these regions are artifacts of the model implementation. While a combination of processes have contributed to the evolution of the Andes, the results presented here show that axial lower crustal flow partitioned by large-scale subduction dynamics is responsible for much of the overall morphology of the central Andes. This also presents a viable and straightforward explanation for the discrepancies between crustal shortening estimates and crustal volume in the Altiplano.

4.1. Crustal Temperature, Strength, and Subduction Geometry

[26] The morphology of the Andes is strongly correlated with the modern dip of the subducting Nazca plate, with a wide plateau over a steeply dipping segment, and with a narrow orogen over flat slab segments. This correlation may arise from the effect of slab dip on the thermal structure of the overriding plate. A gently dipping slab prevents the formation of a mantle wedge and instead places relatively cold oceanic crust at the base of the upper plate. This is thought to result in crust that is colder, stronger, and less ductile above regions of flat slab subduction [*Gutscher*, 2002; *Pérez-Gussinyé et al.*, 2008]. More steeply dipping

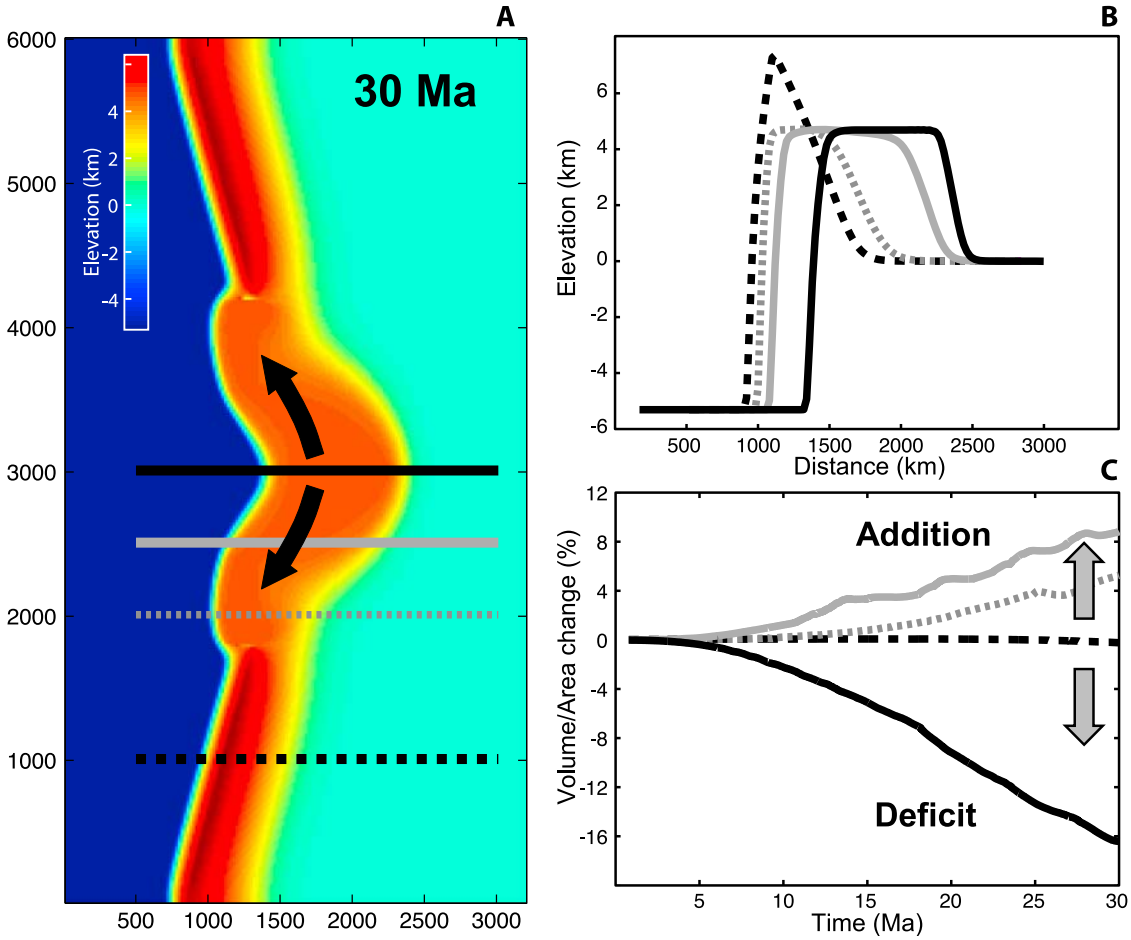

Figure 8. (a) Model topography after 30 Myr and (b) four topographic cross sections showing final topography. Plateau elevations are lower within the central Andes because crust is weaker and flows. (c) Plot showing volume/area change in each cross section through time when compared to the volume/area that is expected from how much convergence and shortening has occurred. This is calculated by taking the crustal volume/area at any point and subtracting by the amount of crustal volume/area expected simply from the amount of shortening experienced. This plot shows the effect of axial lower crustal flow: material flows away from the center toward the north and south, resulting in crustal deficits and volume addition.

slab segments allow the development of a mantle wedge, higher temperatures at the base of the crust, and the introduction of fluids and partial melt [*Gutscher*, 2002]. The higher temperatures and possible introduction of fluids or partial melt will weaken the crust above steeply dipping slab segments and make the lower crust more susceptible to weakening and ductile flow [*Kohlstedt et al.*, 1995; *Rosenberg and Handy*, 2005]. The effect of slab dip can be seen in the pattern in heat flow in the Andes, as several studies find that heat flow is highest in the Altiplano region and drops off to the north and to the south [*Henry and Pollack*, 1988; *Springer and Förster*, 1998]. The correlation that we see between morphology and slab dip as consistent can therefore be explained by cooler temperatures and a stronger lower crust above the flat slab zone blocking longitudinal flow in the lower crust. An important independent constraint on this argument concerning crustal strength in the modern-day Andes comes from effective elastic thickness studies, which find higher elastic thickness in the current flat slab regions and support a connection between slab dip, crustal strength, and susceptibility to crustal flow [*Pérez-Gussinyé et al.*, 2008].

[27] Our most Andean-like results occur under the assumption that something similar to the modern crustal strength variations observed along the Andean margin have been in place throughout most of the orogen's evolution. Recent studies have argued that the present-day flat slab subduction north and south of the Altiplano have developed only in the last 5–10 Myr, in association with an oceanic ridge on the Nazca plate being subducted beneath South America [e.g., *Ramos et al.*, 2002]. Our model results indicate that the axial lower crustal flow that thickens crust north and south of the orocline zone and stops when it reaches the strong flat slab segments occurs in the later stages of orogen evolution, after significant crustal thickening in the center has occurred. We therefore see no significant problem with the argument that

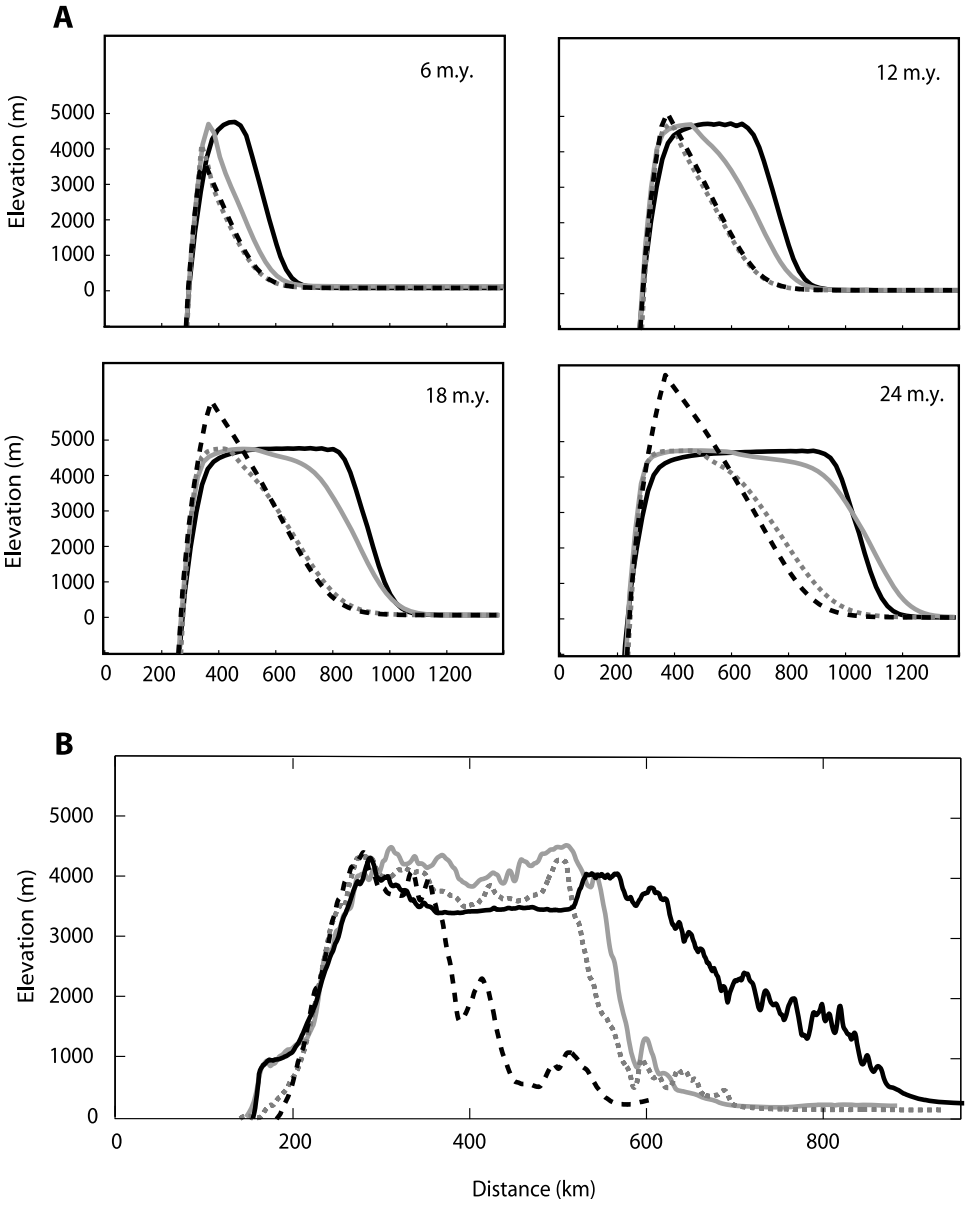

Figure 9. (a) Cross sections of model topography after 6, 12, 18, and 24 Myr of orogen growth. Locations and symbology of cross-section lines are the same as in Figure 7. (b) Mean topography from swath profiles at analogous locations in the Andes.

the modern slab geometry and dip angles may have only been established for the past 5–10 Myr. Related to this discussion is the observation that there are no topographic plateaus in the Andes above the flat slab sections. A basic principle of the model is that plateaus only form when the lower middle crust is weak and can support lower crustal flow. Perhaps the fact that there are no plateaus in the Andes above the modern flat slab sections indicates that (1) only the central Andes are underlain by weak crust or (2) the modern flat slab segments, for whatever reason, have been underlain by stronger lower middle crust for a longer period of time than can be argued to result from oceanic ridges subducting beneath South America. In either case, this may justify keeping those regions strong throughout the entire model evolution as we have, even though the evidence supporting that those regions are strong only applies over the last 5–10 Myr. Prior to 10 Ma, there could have been a different slab geometry.

4.2. Crustal Shortening

[28] The distribution of shortening imposed in our modeling is based on estimates from the central Andes, indicating that the center of the Altiplano has experienced more shortening than the regions to the north and south. There are several proposed explanations for the inferred increase in the amount shortening at the center of the Bolivian orocline.

Table 1. Model Parameters

Variable	Definition of Variables	Value/Initial Value
h	total thickness of the crust	initial h_o = 35 km in continental crust, 1 km in oceanic crust
h_1	maximum thickness of upper crust	50 km
h_{crit}	critical thickness for viscosity transition	65 km
$h - h_1$	approximate thickness of lower crust	15 km
μ_1	viscosity of upper crust	10^{21} Pa s
μ_2	viscosity of lower crust	minimum value 10^{17} Pa s between 14°S and 28°S, 10^{21} Pa s elsewhere
u_{base}	basal velocity in x direction	5–6.5 cm/yr in Nazca Plate, −3 to −1.5 cm/yr in the Brazilian Shield
v_{base}	basal velocity in y direction	0 cm/yr everywhere
u_{suture}	velocity of suture (in x direction)	0.75–3.75 cm/yr
ρ_c	density of the crust	2700 kg/m^3
ρ_m	density of the mantle	3200 kg/m^3
Δt	time step length	0.01 Myr
Δx	grid spacing, equal in x and y directions	20 km

Lamb and Davis [2003] suggest that a drier late Cenozoic climate in the central Andean region resulted in a sediment-starved subduction trench, causing high plate friction and the shear stress needed to support high topography. Another possibility is that an oceanic plateau may have collided with the South American plate, forcing it to shorten as it was dragged under the South American craton [e.g., *Gutscher et al.*, 1999]. Oblique convergence prior to 15 Ma and the geometry of the margin may also have affected the distribution of shortening [*McQuarrie*, 2002]. The correspondence between the location of maximum upper crustal shortening and the center of the steep slab zone hints at a link between shortening and slab geometry.

[29] Regardless of the reasons for the increased shorting in the central Altiplano, our modeling suggests that it is balanced by an outward flow of lower crust and can explain the discrepancy between the central Andes and areas farther north and south. The simple way of looking at our model is that it shows the redistribution of crustal material following an imposed shortening distribution. If shortening is focused in the center and the lower crust is weak, the result is axial flow and redistribution of material north and south. The shortening distribution we assign is essentially a distribution of influxing material, and what we are trying to do is predict the resulting topography/crustal thickness distribution that develops as a consequence. For these purposes, it is the amount of material being added on both sides of the orogen that matters most. We have modeled the fore-arc side of the orogen as an advancing subduction zone with oceanic material scrapping off and being added to the continent and the back-arc side as simple underthrusting. The motion of the South American plate ends up giving the most control over the amount of shortening because once a weak lower crust develops, surface deformation becomes decoupled from the subduction zone boundary at the base of the crust and is no longer greatly affected by the velocity of subduction zone advance.

[30] The addition of crust from the oceanic plate is only a small percentage of material added compared to the subduction zone advance and the underthrusting. For example, our most Andean-like results have a maximum of ~740 km total shortening in the center of the orocline decreasing to ~260 km to the north and south. The oceanic material added over that time is the equivalent of ~50 km of continental crust, ~7% of shortening in the center, and ~20% in the north and south. The measured shortening estimates in the Andes (>300 km for the center and <50 km for the north and 70–120 km for the south) come mainly from the eastern plateau edge and do not account for total shortening across the entire orogen (i.e., from the Nazca plate to the undeformed part of South American plate), as is calculated in the model. Our modeled estimates of maximum shortening, therefore, are in agreement with what is known about total shortening across the Andes.

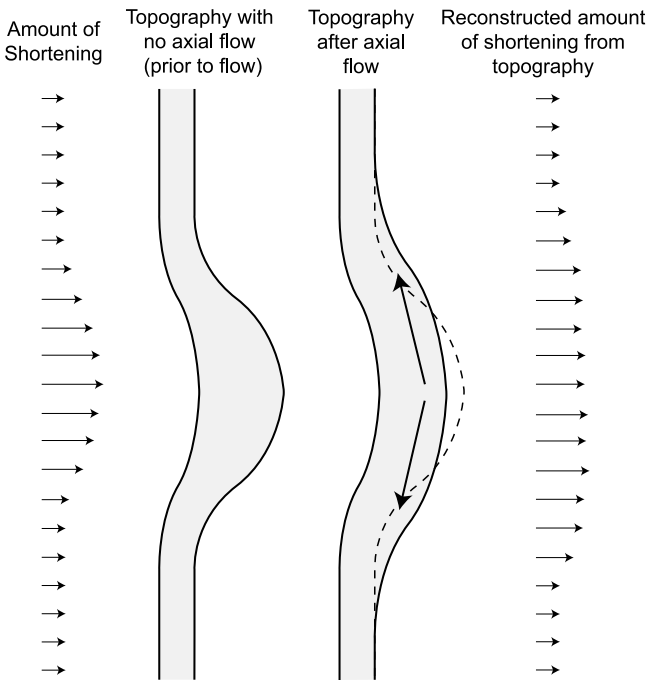

Figure 10. Plan view model for axial lower crustal flow highlighting how the discrepancy between measurements of crustal shortening and the amount needed to account for the current crustal volumes arises. The model predicts that once a weak lower crustal level has developed, significant volumes of material flow along strike, allowing cross-sectional area and orogen widths to be high despite low amounts of crustal shortening experience.

4.3. Effects of Erosion and Lithology

[31] The large-scale symmetry of the Andes, as shown in Figure 3, appears to be unaffected by along-strike variations in lithology and erosion rate. The influence of lower crustal flow is largely confined to regions of thick crust and high topography because flow can only occur in regions with a weak lower crust. However, the slope and width of the lower Andean flanks may be controlled in part by properties and processes in the upper crust. These include erosion and upper crustal lithology. In particular, the width and slope of the Andean flanks below 3 km appear sensitive to lithology and precipitation and erosion rate (Figure 3). A number of studies [*Masek et al.*, 1994; *Horton*, 1999; *Montgomery et al.*, 2001; *Allmendinger et al.*, 1997] have related variations in precipitation, erosion rate, and lithology to variations in morphology along strike in the Andes. Our modeling, and the large-scale symmetry described above, suggests that these processes primarily influence the flanks of the orogen and the regions below ~3 km elevation, while the higher elevation regions and orogen-scale morphology remain largely unaffected.

5. Conclusions

[32] The present morphology and axial symmetry of the Andean belt are independent of widespread variations in along-strike magnitude of upper crustal shortening, bedrock geology, and precipitation. The persistence of axial symmetry despite these variations and the correlation between changes in orogen morphology and the dip of the subducting slab suggest that lithospheric-scale orogenic processes related to slab dip control the regional-scale crustal evolution and morphology of the central Andes.

[33] Our simple, semianalytic, viscous flow model highlights the interaction between slab dip, lower crustal flow, and the development of topography in the Altiplano region of the Andes. As lower crust above the more steeply dipping segment of the subducting slab becomes hot and weak, increased shortening in the center of the Andes drives longitudinal flow of lower crust along strike to the north and south. Longitudinal flow does not penetrate into the flat slab regions, presumably because the crust there is stronger and the lower crust is unable to flow. The redistribution of material results in an apparent discrepancy between local crustal volume and surface shortening. Our results indicate that lower crustal flow exerts a fundamental control on the distribution of topography along and across the central Andes and may explain young (<10 Ma) crustal thickening and surface uplift that has been argued for in some regions.

[34] **Acknowledgments.** This work was supported by the NSF Continental Dynamics program (EAR-0003571), in collaboration with Leigh Royden and Clark Burchfiel at Massachusetts Institute of Technology. We thank Taylor Schildgen for feedback and two anonymous reviewers for constructive and helpful reviews.

References

Allmendinger, R. W., T. E. Jordan, S. M. Kay, and B. L. Isacks (1997), The evolution of the Altiplano-Puna plateau of the central Andes, *Annu. Rev. Earth Planet. Sci.*, *25*, 139–174, doi:10.1146/annurev.earth.25.1.139.

Babeyko, A. Y., S. V. Sobolev, R. B. Trumbull, O. Oncken, and L. L. Lavier (2002), Numerical models of crustal scale convection and partial melting beneath the Altiplano-Puna plateau, *Earth Planet. Sci. Lett.*, *199*, 373–388, doi:10.1016/S0012-821X(02)00597-6.

Barke, R., and S. Lamb (2006), Late Cenozoic uplift of the Eastern Cordillera, Bolivian Andes, *Earth Planet. Sci. Lett.*, *249*, 350–367, doi:10.1016/j.epsl.2006.07.012.

Barnes, J. B., T. A. Ehlers, N. McQuarrie, P. B. O'Sullivan, and J. D. Pelletier (2006), Eocene to recent variations in erosion across the central Andean fold-thrust belt, northern Bolivia: Implications for plateau evolution, *Earth Planet. Sci. Lett.*, *248*, 118–133, doi:10.1016/j.epsl.2006.05.018.

Beaumont, C., M. Nguyen, R. A. Jamieson, and S. Ellis (2006), Crustal flow modes in large hot orogens, in *Channel Flow, Ductile Extrusion and Exhumation in Continental Collision Zones*, edited by R. D. Law, M. Searle, and L. Godin, *Geol. Soc. Spec. Publ.*, *268*, 91–145, doi:10.1144/GSL.SP.2006.268.01.05.

Beck, S. L., G. Zandt, S. C. Myers, T. C. Wallace, P. G. Silver, and L. Drake (1996), Crustal thickness variations in the central Andes, *Geology*, *24*(5), 407–410, doi:10.1130/0091-7613(1996)024<0407:CTVITC>2.3.CO;2.

Bird, P. (1991), Lateral extrusion of lower crust from under high topography, in the isostatic limit, *J. Geophys. Res.*, *96*, 10,275–10,286, doi:10.1029/91JB00370.

Cahill, T., and B. L. Isacks (1992), Seismicity and shape of the subducted Nazca plate, *J. Geophys. Res.*, *97*, 17,503–17,529, doi:10.1029/92JB00493.

Clark, M., and L. Royden (2000), Topographic ooze: Building the eastern margin of Tibet by lower crustal flow, *Geology*, *28*(8), 703–706, doi:10.1130/0091-7613(2000)28<703:TOBTEM>2.0.CO;2.

Cook, K. L., and L. H. Royden (2008), The influence of crustal strength variations on the development of collisional plateaus, with application to Tibet, *J. Geophys. Res.*, *113*, B08407, doi:10.1029/2007JB005457.

DeMets, C., R. G. Gordon, D. F. Argus, and S. Stein (1994), Effect of recent revisions to the geomagnetic reversal time scale on estimates of current plate motions, *Geophys. Res. Lett.*, *21*(20), 2191–2194, doi:10.1029/94GL02118.

Ege, H., E. R. Sobel, E. Scheuber, and V. Jacobshagen (2007), Exhumation history of the southern Altiplano plateau (southern Bolivia) constrained by apatite fission track thermo-chronology, *Tectonics*, *26*, TC1004, doi:10.1029/2005TC001869.

Ehlers, T. A., and C. J. Poulsen (2009), Influence of Andean uplift on climate and paleoaltimetry estimates, *Earth Planet. Sci. Lett.*, *281*, 238–248, doi:10.1016/j.epsl.2009.02.026.

Elger, K., O. Oncken, and J. Glodny (2005), Plateau-style accumulation of deformation: Southern Altiplano, *Tectonics*, *24*, TC4020, doi:10.1029/2004TC001675.

Garzione, C. N., P. Molnar, J. C. Libarkin, and B. J. MacFadden (2006), Rapid late Miocene rise of the Bolivian Altiplano: Evidence for removal of mantle lithosphere, *Earth Planet. Sci. Lett.*, *241*, 543–556, doi:10.1016/j.epsl.2005.11.026.

Gephart, J. W. (1994), Topography and subduction geometry in the central Andes: Clues to the mechanics of a noncollisional orogen, *J. Geophys. Res.*, *99*, 12,279–12,288, doi:10.1029/94JB00129.

Ghosh, P., C. N. Garzione, and J. M. Eiler (2006), Rapid uplift of the Altiplano revealed through ^{13}C–^{18}O bonds in paleosol carbonates, *Science*, *311*, 511–515, doi:10.1126/science.1119365.

Gillis, R. J., B. K. Horton, and M. Grove (2006), Thermochronology, geochronology, and upper crustal structure of the Cordillera Real: Implications for Cenozoic exhumation history of the central Andean Plateau, *Tectonics*, *25*, TC6007, doi:10.1029/2005TC001887.

Gregory-Wodzicki, K. M. (2000), Uplift history of the central and northern Andes: A review, *Geol. Soc. Am. Bull.*, *112*(7), 1091–1105, doi:10.1130/0016-7606(2000)112<1091:UHOTCA>2.0.CO;2.

Gubbels, T. L., B. L. Isacks, and E. Farrar (1993), High-level surfaces, plateau uplift, and foreland development, Bolivian central Andes, *Geology*, *21*(8), 695–698, doi:10.1130/0091-7613(1993)021<0695:HLSPUA>2.3.CO;2.

Gutscher, M. A. (2002), Andean subduction styles and their effect on thermal structure and interplate coupling, *J. South Am. Earth Sci.*, *15*, 3–10, doi:10.1016/S0895-9811(02)00002-0.

Gutscher, M. A., J. L. Olivet, D. Aslanian, J. P. Eissen, and R. Maury (1999), The "lost Inca Plateau": Cause of flat subduction beneath Peru?, *Earth Planet. Sci. Lett.*, *171*, 335–341, doi:10.1016/S0012-821X(99)00153-3.

Henry, S. G., and H. N. Pollack (1988), Terrestrial heat flow above the Andean subduction zone in Bolivia and Peru, *J. Geophys. Res.*, *93*, 15,153–15,162, doi:10.1029/JB093iB12p15153.

Hindle, D., J. Kley, O. Oncken, and S. Sobolev (2005), Crustal balance and crustal flux from shortening estimates in the central Andes, *Earth Planet. Sci. Lett.*, *230*, 113–124, doi:10.1016/j.epsl.2004.11.004.

Horton, B. K. (1999), Erosional control on the geometry and kinematics of thrust belt development in the central Andes, *Tectonics*, *18*, 1292–1304, doi:10.1029/1999TC900051.

Husson, L., and T. Sempere (2003), Thickening the Altiplano crust by gravity-driven crustal channel flow, *Geophys. Res. Lett.*, *30*(5), 1243, doi:10.1029/2002GL016877.

Isacks, B. L. (1988), Uplift of the Central Andean plateau and the bending of the Bolivian Orocline, *J. Geophys. Res.*, *93*, 3211–3231, doi:10.1029/JB093iB04p03211.

Jordan, T. E., B. L. Isacks, R. W. Allmendinger, J. A. Brewer, V. A. Ramos, and C. J. Ando (1983), Andean tectonics related to geometry of subducted Nazca plate, *Geol. Soc. Am. Bull.*, *94*, 341–361, doi:10.1130/0016-7606(1983)94<341:ATRTGO>2.0.CO;2.

Kley, J., and C. R. Monaldi (1998), Tectonic shortening and crustal thickness in the central Andes: How good is the correlation?, *Geology*, *26*(8), 723–726, doi:10.1130/0091-7613(1998)026<0723:TSACTI>2.3.CO;2.

Kohlstedt, D. L., B. Evans, and S. J. Mackwell (1995), Strength of the lithosphere: Constraints imposed by laboratory experiments, *J. Geophys. Res.*, *100*, 17,587–17,602, doi:10.1029/95JB01460.

Lamb, S., and P. Davis (2003), Cenozoic climate change as a possible cause for the rise of the Andes, *Nature*, *425*, 792–797, doi:10.1038/nature02049.

Lamb, S., and L. Hoke (1997), Origin of the high plateau in the central Andes, Bolivia, South America, *Tectonics*, *16*(4), 623–649, doi:10.1029/97TC00495.

Masek, J. G., B. L. Isacks, T. L. Gubbels, and E. J. Fielding (1994), Erosion and tectonics of margins of continental plateaus, *J. Geophys. Res.*, *99*, 13,941–13,956, doi:10.1029/94JB00461.

McQuarrie, N. (2002), Initial plate geometry, shortening variations, and evolution of the Bolivian Orocline, *Geology*, *30*(10), 867–870, doi:10.1130/0091-7613(2002)030<0867:IPGSVA>2.0.CO;2.

McQuarrie, N., J. B. Barnes, and T. A. Ehlers (2008), Geometric, kinematic, and erosional history of the central Andean Plateau, Bolivia, *Tectonics*, *27*, TC3007, doi:10.1029/2006TC002054.

Montgomery, D. R., G. Balco, and S. D. Willet (2001), Climate, tectonics, and the morphology of the Andes, *Geology*, *29*(7), 579–582, doi:10.1130/0091-7613(2001)029<0579:CTATMO>2.0.CO;2.

Norabuena, E., L. Leffler-Griffin, A. Mao, T. Dixon, S. Stein, I. Selwyn Sacks, L. Ocola, and M. Ellis (1998), Space geodetic observations of Nazca–South America convergence across the central Andes, *Science*, *279*, 358–362, doi:10.1126/science.279.5349.358.

Pérez-Gussinyé, M., A. R. Lowry, J. Phipps Morgan, and A. Tassara (2008), Effective elastic thickness variations along the Andean margin and their relationship to subduction geometry, *Geochem. Geophys. Geosyst.*, *9*, Q02003, doi:10.1029/2007GC001786.

Peterson, T. C., and R. S. Vose (1997), An overview of the Global Historical Climatology Network temperature data base, *Bull. Am. Meteorol. Soc.*, *78*, 2837–2849, doi:10.1175/1520-0477(1997)078<2837:AOOTGH>2.0.CO;2.

Ramos, V. A., E. O. Cristallini, and D. J. Pérez (2002), The Pampean flat-slab of the central Andes, *J. South Am. Earth Sci.*, *15*, 59–78, doi:10.1016/S0895-9811(02)00006-8.

Rosenberg, C., and M. Handy (2005), Experimental deformation of partially melted granite revisited: Implications for the continental crust, *J. Metamorph. Geol.*, *23*, 19–28, doi:10.1111/j.1525-1314.2005.00555.x.

Royden, L. H. (1996), Coupling and decoupling of crust and mantle in convergent orogens: Implications for strain partitioning in the crust, *J. Geophys. Res.*, *101*, 17,679–17,705, doi:10.1029/96JB00951.

Schenk, C. J., R. J. Viger, and C. P. Anderson (1998), Maps showing geology, oil and gas fields, and geologic provinces of the South America region, *U.S. Geol. Surv. Open File Rep.*, *97-470D*.

Schildgen, T. F., K. V. Hodges, K. X. Whipple, P. W. Reiners, and M. S. Pringle (2007), Uplift of the western Altiplano revealed through canyon incision history, southern Peru, *Geology*, *35*(6), 523–526, doi:10.1130/G23532A.1.

Sempere, T., et al. (2002), Late Permian–Middle Jurassic lithospheric thinning in Peru and Bolivia, and its bearing on Andean-age tectonics, *Tectonophysics*, *345*, 153–181, doi:10.1016/S0040-1951(01)00211-6.

Shen, F., L. H. Royden, and B. C. Burchfiel (2001), Large-scale crustal deformation of the Tibetan Plateau, *J. Geophys. Res.*, *106*, 6793–6816, doi:10.1029/2000JB900389.

Springer, M., and A. Förster (1998), Heat-flow density across the central Andean subduction zone, *Tectonophysics*, *291*, 123–139, doi:10.1016/S0040-1951(98)00035-3.

Vanderhaeghe, O., S. Medvedev, P. Fullsack, C. Beaumont, and R. A. Jamieson (2003), Evolution of orogenic wedges and continental plateaux: Insights from crustal thermal-mechanical models overlying subducting mantle lithosphere, *Geophys. J. Int.*, *153*, 27–51, doi:10.1046/j.1365-246X.2003.01861.x.

Victor, P., O. Oncken, and J. Glodny (2004), Uplift of the western Altiplano plateau: Evidence from the Precordillera between 20 and 21°S (northern Chile), *Tectonics*, *23*, TC4004, doi:10.1029/2003TC001519.

Yang, Y., M. Liu, and S. Stein (2003), A 3-D geodynamic model of lateral crustal flow during Andean mountain building, *Geophys. Res. Lett.*, *30*(10), 2093, doi:10.1029/2003GL018308.

K. L. Cook, Department of Geosciences, National Taiwan University, No. 1, Sec. 4, Roosevelt Rd., Taipei, 106, Taiwan.

W. B. Ouimet, Department of Geology, Amherst College, 11 Barren Hill Rd., Amherst, MA 01002, USA. (willouimet@gmail.com)